

Faddeev-type calculation of (d, n) transfer reactions in three-body nuclear systems

A. Deltuva*

Institute of Theoretical Physics and Astronomy, Vilnius University, A. Goštauto 12, LT-01108 Vilnius, Lithuania

(Received October 11, 2015)

Exact Faddeev-type three-body equations are applied to the study of the proton transfer reactions (d, n) in the system consisting of a nuclear core and two nucleons. The integral equations for the three-body transition operators are solved in the momentum-space framework including the Coulomb interaction via the screening and renormalization method. For a weakly bound final nucleus the calculation of the (d, n) reaction is more demanding in terms of the screening radius as compared to the (d, p) reaction. Well converged differential cross section results are obtained for ${}^7\text{Be}(d, n){}^8\text{B}$, ${}^{12}\text{C}(d, n){}^{13}\text{N}$, and ${}^{16}\text{O}(d, n){}^{17}\text{F}$ reactions. A comparison with the corresponding (d, p) reactions is made. The calculations fail to reproduce the shape of the angular distribution for reactions on ${}^{12}\text{C}$ but provide quite successful description for reactions on ${}^{16}\text{O}$, especially for the transfer to the ${}^{17}\text{F}$ excited state $1/2^+$ when using a nonlocal optical potential.

PACS numbers: 24.10.-i, 21.45.-v, 25.45.Hi, 25.40.Hs

I. INTRODUCTION

Although there is a long history of nuclear reaction calculations using three-body models [1, 2], the rigorous Faddeev-type scattering theory [3, 4] was practically applied to nuclear reaction problem only in the last decade [5, 6]. Despite being theoretically most complicated and computationally more expensive than traditional approximate three-body reactions methods, the Faddeev formalism has an advantage that, once numerically well-converged results are obtained, the discrepancies with the experimental data can be attributed to the shortcomings of the used potentials or to the inadequacy of the three-body model. The numerical calculations [5, 6] have been performed using the Alt-Grassberger-Sandhas (AGS) integral equations for transition operators [4] that were solved in the momentum-space framework; the Coulomb interaction was included via the screening and renormalization method [7–9]. So far the applications of Faddeev/AGS equations are limited to three-body systems made of a proton (p), neutron (n), and nuclear core (A). With A most often being one of ${}^{10}\text{Be}$, ${}^{12}\text{C}$, ${}^{14}\text{C}$, or ${}^{16}\text{O}$, reactions initiated by the collisions of the deuteron (d) with the nucleus A and of the proton with the bound system (An) have been studied, including the elastic proton and deuteron scattering, i.e., (p, p) and (d, d) processes, deuteron breakup (d, pn) and one-neutron removal (p, pn) , deuteron stripping (d, p) and pickup (p, d) , and, to a lesser extent, the charge-exchange reaction (p, n) . However, to date there are no deuteron stripping (d, n) and its time-reverse (n, d) reaction calculations in three-body Faddeev/AGS equation framework. Among the two the (d, n) process is especially important since it may be used for the creation and study of weakly bound core plus valence proton (Ap) systems such as one proton halo nucleus ${}^8\text{B}$. Therefore the aim of the present work is to

extend the rigorous three-body Faddeev/AGS framework and to apply it to the study of (d, n) reactions.

In Sec. II the Faddeev/AGS formalism is recalled and specific aspects of (d, n) reaction calculations are pointed out. In Sec. III physics results are presented for the (d, n) reactions on ${}^7\text{Be}$, ${}^{12}\text{C}$, and ${}^{16}\text{O}$ nuclei; for the latter two the comparison with the corresponding (d, p) reactions is made as well; the results for the elastic scattering, extensively studied in previous works [5, 6, 10], are not shown. The summary is given in Sec. IV.

II. THEORETICAL FRAMEWORK

The AGS formalism is an integral equation formulation of the exact three-body scattering theory. Instead of the wave function it deals with transition operators that contain the full physical information about the considered process. The AGS integral equations are most convenient to solve in the momentum-space representation. The standard AGS formalism assumes short-range potentials within the three pairs of particles. This condition is fulfilled by the nuclear interactions v_A , v_p , and v_n that, in the odd-man-out notation, denote p - n , n - A , and A - p potentials, respectively. However, the proton-core Coulomb repulsion w_n , in the coordinate space given as $w_n(r) = Z\alpha_e/r$ with Z being the charge number of nucleus A and $\alpha_e \approx 1/137$ the fine structure constant, is of the long range. Nevertheless, w_n can be included rigorously using the screening and renormalization method [7–9]. For this purpose the screened Coulomb potential

$$w_{nR}(r) = w_n(r)e^{-(r/R)^{\bar{n}}}, \quad (1)$$

where R is the screening radius and \bar{n} is the screening smoothness parameter, is added to the nuclear one allowing the standard scattering theory to be applied for the sum $v_n + w_{nR}$.

Via the Lippmann-Schwinger integral equation the pair potentials yield the corresponding two-particle tran-

* arnoldas.deltuva@tfai.vu.lt

sition operators

$$T_A = v_A + v_A G_0 T_A, \quad (2a)$$

$$T_p = v_p + v_p G_0 T_p, \quad (2b)$$

$$T_n^{(R)} = v_n + w_{nR} + (v_n + w_{nR}) G_0 T_n^{(R)}. \quad (2c)$$

Here $G_0 = (E + i0 - H_0)^{-1}$ is the free resolvent at the energy E available for the relative three-body motion, and H_0 is the respective three-body kinetic energy operator. The two-body transition operators, when iterated to all orders via AGS equations, lead to the three-body transition operators. The deuteron-nucleus scattering process is described by the set

$$U_{AA}^{(R)} = T_p G_0 U_{pA}^{(R)} + T_n^{(R)} G_0 U_{nA}^{(R)}, \quad (3a)$$

$$U_{pA}^{(R)} = G_0^{-1} + T_n^{(R)} G_0 U_{nA}^{(R)} + T_A G_0 U_{AA}^{(R)}, \quad (3b)$$

$$U_{nA}^{(R)} = G_0^{-1} + T_A G_0 U_{AA}^{(R)} + T_p G_0 U_{pA}^{(R)}. \quad (3c)$$

Through $T_n^{(R)}$ also the three-body transition operators acquire the dependence on the A - p Coulomb screening radius R . The transition amplitudes for the two-cluster reactions initiated by the $d+A$ collisions are determined by the on-shell matrix elements of three-body transition operators between the respective initial and final two-cluster channel states $|\Phi_A(\mathbf{q}_A)\rangle = |\phi_A\rangle|\mathbf{q}_A\rangle$, $|\Phi_p(\mathbf{q}_p)\rangle = |\phi_p\rangle|\mathbf{q}_p\rangle$, and $|\Phi_n^{(R)}(\mathbf{q}_n)\rangle = |\phi_n^{(R)}\rangle|\mathbf{q}_n\rangle$. Here $|\mathbf{q}_\alpha\rangle$ is a free wave for the α spectator-pair relative motion with the momentum \mathbf{q}_α while $|\phi_A\rangle$, $|\phi_p\rangle$, and $|\phi_n^{(R)}\rangle$ are two-body bound state wave functions for the (pn) , (nA) , and (Ap) subsystems calculated with the potentials v_A , v_p , and $v_n + w_{nR}$, respectively. The dependence on the other discrete quantum numbers is suppressed in the notation. None of the matrix elements $\langle\Phi_A(\mathbf{q}'_A)|U_{AA}^{(R)}|\Phi_A(\mathbf{q}_A)\rangle$, $\langle\Phi_p(\mathbf{q}_p)|U_{pA}^{(R)}|\Phi_A(\mathbf{q}_A)\rangle$, $\langle\Phi_n^{(R)}(\mathbf{q}_n)|U_{nA}^{(R)}|\Phi_A(\mathbf{q}_A)\rangle$ has the $R \rightarrow \infty$ limit, however, after the renormalization with the appropriate (diverging as well) phase factors $Z_{\alpha R}$ the infinite R limit exists [7–9] and corresponds to the physical transition amplitudes

$$\begin{aligned} \mathcal{T}_{AA}(\mathbf{q}'_A, \mathbf{q}_A) &= t_A^C(\mathbf{q}'_A, \mathbf{q}_A) + \lim_{R \rightarrow \infty} [Z_{AR}^{-\frac{1}{2}}(q'_A) \langle\Phi_A(\mathbf{q}'_A)| \\ &\quad \times (U_{AA}^{(R)} - t_A^R) |\Phi_A(\mathbf{q}_A)\rangle Z_{AR}^{-\frac{1}{2}}(q_A)], \end{aligned} \quad (4a)$$

$$\begin{aligned} \mathcal{T}_{pA}(\mathbf{q}_p, \mathbf{q}_A) &= \lim_{R \rightarrow \infty} [Z_{pR}^{-\frac{1}{2}}(q_p) \langle\Phi_p(\mathbf{q}_p)| \\ &\quad \times U_{pA}^{(R)} |\Phi_A(\mathbf{q}_A)\rangle Z_{AR}^{-\frac{1}{2}}(q_A)], \end{aligned} \quad (4b)$$

$$\mathcal{T}_{nA}(\mathbf{q}_n, \mathbf{q}_A) = \lim_{R \rightarrow \infty} [\langle\Phi_n^{(R)}(\mathbf{q}_n)|U_{nA}^{(R)}|\Phi_A(\mathbf{q}_A)\rangle Z_{AR}^{-\frac{1}{2}}(q_A)]. \quad (4c)$$

In the case of the elastic scattering the longest-range screened Coulomb contribution t_A^R , corresponding to the Coulomb interaction between the nucleus and the center-of-mass (c.m.) of the deuteron, is separated from $U_{AA}^{(R)}$ and renormalized analytically in the infinite R limit, leading to the standard Rutherford amplitude $t_A^C(\mathbf{q}'_A, \mathbf{q}_A)$ [7].

All remaining terms have to be calculated numerically, but owing to their short-range nature, the convergence with R is quite fast as will be demonstrated. Since the AGS equations are solved in the partial-wave representation, the renormalization factors are most conveniently calculated as

$$Z_{\alpha R}(q_\alpha) = e^{-2i[\sigma_{\alpha,L}^C(q_\alpha) - \eta_{\alpha,L}^R(q_\alpha)]}, \quad (5)$$

where the full and screened Coulomb phase shifts $\sigma_{\alpha,L}^C(q_\alpha)$ and $\eta_{\alpha,L}^R(q_\alpha)$ correspond to the relative motion with the angular momentum L between the particle α and c.m. of the remaining pair.

Equation (4c) takes into account that there is no Coulomb interaction between the neutron and the (Ap) pair, i.e., $Z_{nR}(q_n) = 1$ and the final $n + (Ap)$ state is not distorted by the Coulomb force. However, in contrast to other channel states, the bound state $|\phi_n^{(R)}\rangle$ is affected by the screened Coulomb interaction. Due to $|\phi_n^{(R)}\rangle$ one may expect for observables of the (d, n) reaction a different convergence rate with increasing R as compared to the (d, p) reaction. These differences will be studied in the next section.

III. RESULTS

As already mentioned, the AGS integral equations (3) are solved numerically in the momentum-space partial-wave basis. Typically, the potentials v_A , v_p , and v_n are allowed to act in the partial waves with the respective pair orbital angular momentum l_α up to 2, 5, and 10; the latter is not really needed for v_n but is necessary for the screened Coulomb potential w_{nR} . Three-body states with the total angular momentum up to $J \leq 20$ are included. With these cutoffs well converged results are obtained.

The p - n potential v_A is taken to be the realistic CD Bonn potential [11]; the results show very little sensitivity to the choice of v_A provided it remains a realistic high-precision potential. This is not so for the nucleon-core potentials v_p and v_n . The predictions are therefore obtained using several parametrizations of the nucleon-core optical potential, namely, those of Watson (W) [12], Chapel Hill 89 (CH89) [13], Koning-Delaroche (KD) [14], and the nonlocal (NL) potential introduced by Giannini and Ricco [15] but with the parameters readjusted in Ref. [10] to the experimental data for the nucleon scattering from ^{12}C and ^{16}O . For this reason the NL potential is not applied to the $d + ^7\text{Be}$ reaction. Note that CH89 and KD potentials were originally fitted to heavier nuclei $A \geq 24$ data but nowadays are often used also for light nuclei such as isotopes of carbon or beryllium [16] and provide quite a reasonable description. The Watson potential was designed for the light p -shell nuclei but it is rather old and may lack accuracy. The NL parameters are energy-independent, while for local energy-dependent potentials they are taken at half energy of the deuteron

TABLE I. Valence nucleon quantum numbers in the spectroscopic nlj notation, the binding energies ϵ_α , and the potential strengths V_c for the considered final-state nuclei. For $^{17}\text{F}(1/2^+)$ and $^{17}\text{O}(1/2^+)$ the Pauli forbidden $1s_{1/2}$ state is projected out.

	valence	$\epsilon_\alpha(\text{MeV})$	$V_c(\text{MeV})$
$^8\text{B}(2^-)$	$1p_{3/2}$	0.137	43.074
$^{13}\text{N}(1/2^-)$	$1p_{1/2}$	1.944	44.361
$^{13}\text{C}(1/2^-)$	$1p_{1/2}$	4.946	44.365
$^{17}\text{F}(5/2^+)$	$1d_{5/2}$	0.600	52.858
$^{17}\text{F}(1/2^+)$	$2s_{1/2}$	0.105	53.002
$^{17}\text{O}(5/2^+)$	$1d_{5/2}$	4.143	52.813
$^{17}\text{O}(1/2^+)$	$2s_{1/2}$	3.272	53.167

beam $E_d/2$ as proposed in Refs. [1, 17]. In the partial waves with the core-nucleon bound state the potentials v_p and v_n must be real and energy-independent. In the coordinate space they are taken to have central and spin-orbit parts, i.e.,

$$v_\alpha(r) = -V_c f(r, R, a) + \boldsymbol{\sigma} \cdot \mathbf{L} V_{so} \frac{2}{r} \frac{d}{dr} f(r, R, a), \quad (6)$$

with $f(r, R, a) = [1 + \exp((r - R)/a)]^{-1}$ and standard values for the parameters $R = r_0 A^{1/3}$, $r_0 = 1.25$ fm, $a = 0.65$ fm, and $V_{so} = 6.0 \text{ MeV} \cdot \text{fm}^2$, while V_c is adjusted to reproduce the desired binding energy. For all considered final-state nuclei the binding energies ϵ_α , the valence particle quantum numbers, and the respective V_c values are collected in Table I. Since the excitations of the core A are not taken into account, all these nuclei are single-component states with the respective spectroscopic factor being unity.

The choice to fix the parameters of the local optical potential at $E_d/2$ was proposed in Refs. [1, 17] and has been used widely, but recently has been criticized in Ref. [18] from the adiabatic distorted-wave approximation (ADWA) point of view, suggesting the energy that is higher by about 40 MeV. However, such a high value $E_d/2 + 40$ MeV at low E_d is not consistent with the three-body Faddeev/AGS formalism where, when integrating over the spectator momentum q_α , the two-body subsystem energy $E_\alpha = E - q_\alpha^2/2M_\alpha$ runs from the maximal value $E = E_d A/(A + 2) - 2.225$ MeV to $-\infty$. Although Ref. [6] took this aspect into account and used an extended Faddeev/AGS formalism allowing optical potentials that vary with the two-body subsystem energy, the standard calculations in the present work are performed with optical potentials taken at a fixed energy in order to have a single three-body Hamiltonian and thereby preserve a Hamiltonian theory. For the same reason the binding potentials (6) are chosen energy-independent as well. These inconsistencies and ambiguities arise due to the reduction of the $(A + 2)$ body problem to the three-body problem. The related uncertainties in the present results will be discussed at the end of this section.

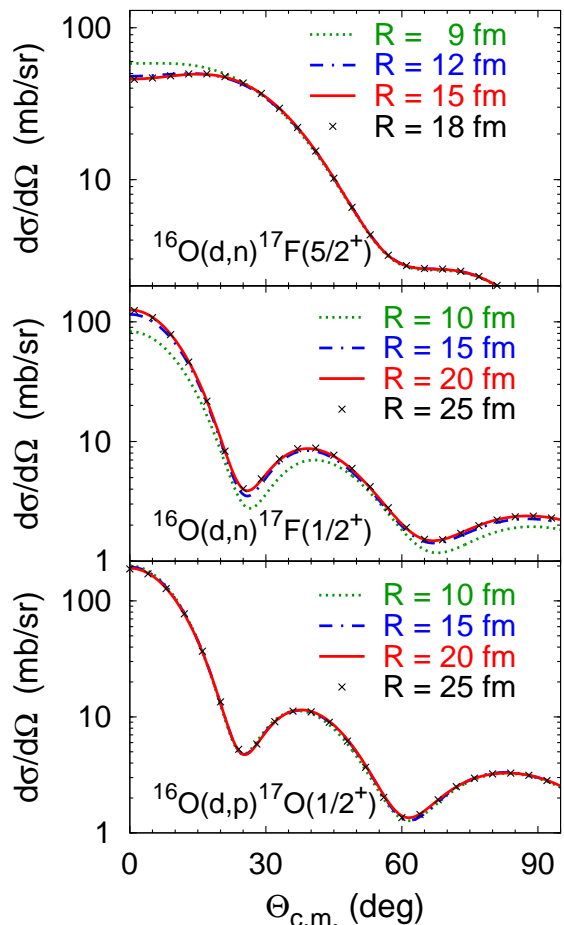


FIG. 1. (Color online) Differential cross section for $^{16}\text{O}(d,n)^{17}\text{F}$ and $^{16}\text{O}(d,p)^{17}\text{O}$ transfer reactions at $E_d = 12$ MeV. Results obtained with different values of the Coulomb screening radius R are compared. The screening smoothness parameter $\bar{n} = 8$.

To demonstrate the numerical reliability of the proposed calculational scheme for (d, n) reactions, the convergence with the Coulomb screening radius R is studied in Fig. 1. As a working example the reactions with the strongest Coulomb interaction, i.e., $^{16}\text{O}(d, n)^{17}\text{F}$, are chosen. Since ^{17}F has ground and excited states, the convergence is checked for different values of the orbital angular momentum l_n and of the binding energy ϵ_n for the bound proton-core pair as listed in Table I. In the case of the $^{17}\text{F}(1/2^+)$ excited state, owing to its very weak binding $\epsilon_n = 0.105$ MeV, a more significant sensitivity to the Coulomb screening radius R may be expected. This is indeed so as Fig. 1 shows for the differential cross section $d\sigma/d\Omega$ as a function of the c.m. scattering angle $\Theta_{\text{c.m.}}$ at deuteron beam energy $E_d = 12$ MeV. While for the transfer to the ground state $^{17}\text{F}(5/2^+)$ the R -independence is established at $R > 12$ fm, the same level of convergence for the transfer to the excited state $^{17}\text{F}(1/2^+)$ is reached only at $R \geq 20$ fm. For comparison, $d\sigma/d\Omega$ is presented

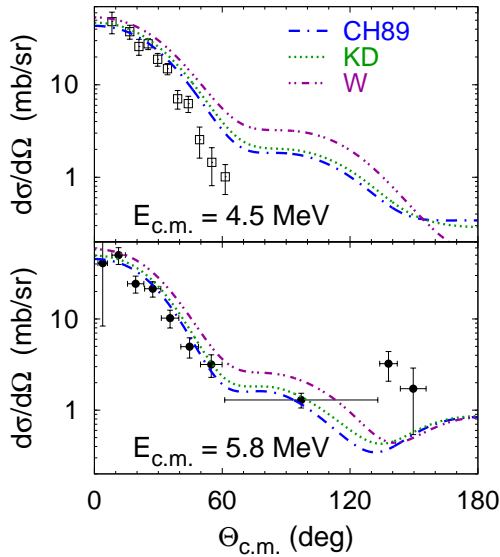


FIG. 2. (Color online) Differential cross section for the ${}^7\text{Be}(d,n){}^8\text{B}$ transfer reaction at $E_{c.m.} = 4.5$ and 5.8 MeV. Predictions obtained using Chappel Hill 89 (dashed-dotted curves), Koning-Delaroché (dotted curves), and Watson (dashed-double-dotted curves) optical potentials are compared with the experimental data from Refs. [19] (5.8 MeV) and [20] (4.5 MeV).

also for the ${}^{16}\text{O}(d,p){}^{17}\text{O}(1/2^+)$ reaction where the final-channel two-particle bound state is Coulomb-free but the two-cluster scattering state has to be renormalized. The convergence with R is considerably faster in this case. Thus, compared to (d,p) the calculation of (d,n) reactions is more demanding in terms of the screening radius but, nevertheless, well-converged results are obtained.

In the following the physics results for ${}^7\text{Be}(d,n){}^8\text{B}$, ${}^{12}\text{C}(d,n){}^{13}\text{N}$, and ${}^{16}\text{O}(d,n){}^{17}\text{F}$ reactions are presented and compared with the experimental data.

I start with the ${}^7\text{Be}(d,n){}^8\text{B}$ reaction where the experimental data are rather scarce and a bit contradictory [19, 20]. Differential cross section results at $d + {}^7\text{Be}$ kinetic c.m. energy of 4.5 and 5.8 MeV obtained using CH89, KD, and W optical potential models are given in Fig. 2. The predictions of CH89 are closest to the data but one should keep in mind that this potential as well as KD is not fitted to the nucleon- ${}^7\text{Be}$ data. All calculations reproduce reasonably the angular shape of $d\sigma/d\Omega$ but overpredict its magnitude. This is not unexpected given the existence of low-energy excitations of the ${}^7\text{Be}$ core that are not taken into account in the present calculations. Relying on the analogy with the ${}^{10}\text{Be}(d,p){}^{11}\text{Be}$ reactions [21] one may expect that including the ${}^7\text{Be}$ core excitation would lead to the reduction of the transfer cross section, at least at forward angles.

Next I show in Fig. 3 the differential cross section for the ${}^{12}\text{C}(d,n){}^{13}\text{N}$ transfer reaction at $E_d = 7, 12, 18,$ and 25 MeV. The used optical potentials are CH89, KD, and NL. For all of them the angular shape fails in accounting

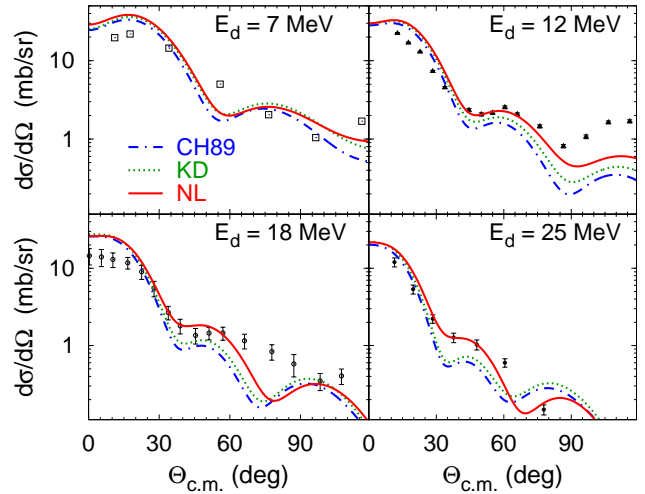


FIG. 3. (Color online) Differential cross section for the ${}^{12}\text{C}(d,n){}^{13}\text{N}$ reaction at $7, 12, 18,$ and 25 MeV deuteron energy. Predictions obtained using the Chappel Hill 89 (dashed-dotted curves), Koning-Delaroché (dotted curves), and non-local (solid curves) optical potentials are compared with the experimental data from Refs. [22] (7 MeV), [23] (12 MeV), [24] (18 MeV), and [25] (25 MeV).

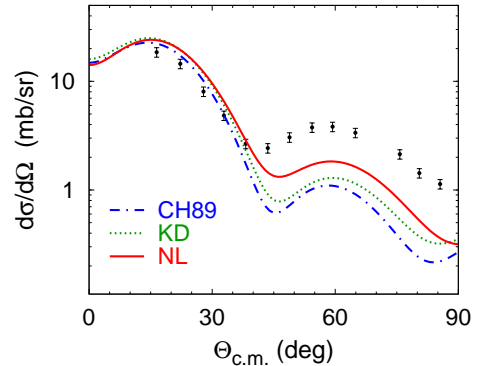


FIG. 4. (Color online) Differential cross section for the ${}^{12}\text{C}(d,p){}^{13}\text{C}$ reaction at 12 MeV deuteron energy. Curves are as in Fig. 3, and the experimental data are from Ref. [26].

for the experimental data: the data points from Refs. [22–25] are overestimated at forward angles $\Theta_{c.m.} < 30^\circ$ and underestimated at large angles $\Theta_{c.m.} > 90^\circ$. This discrepancy is comparable with the one in the ${}^{12}\text{C}(d,p){}^{13}\text{C}$ reaction [26], displayed in Fig. 4. A somehow similar discrepancy, i.e., overprediction at small angles and underprediction of the data at larger angles, was observed also at higher energies in the ${}^{12}\text{C}(d,p){}^{13}\text{C}$ reaction, but only for the ${}^{13}\text{C}$ ground state $1/2^-$; the agreement for the transfer to ${}^{13}\text{C}$ excited states $1/2^+$ and $5/2^+$ was significantly better, especially when using the nonlocal optical potential [10]. In this view the failure of the calculations to reproduce the ${}^{12}\text{C}(d,n){}^{13}\text{N}$ data is not unexpected.

Finally I consider the ${}^{16}\text{O}(d,n){}^{17}\text{F}$ reactions. Unfor-

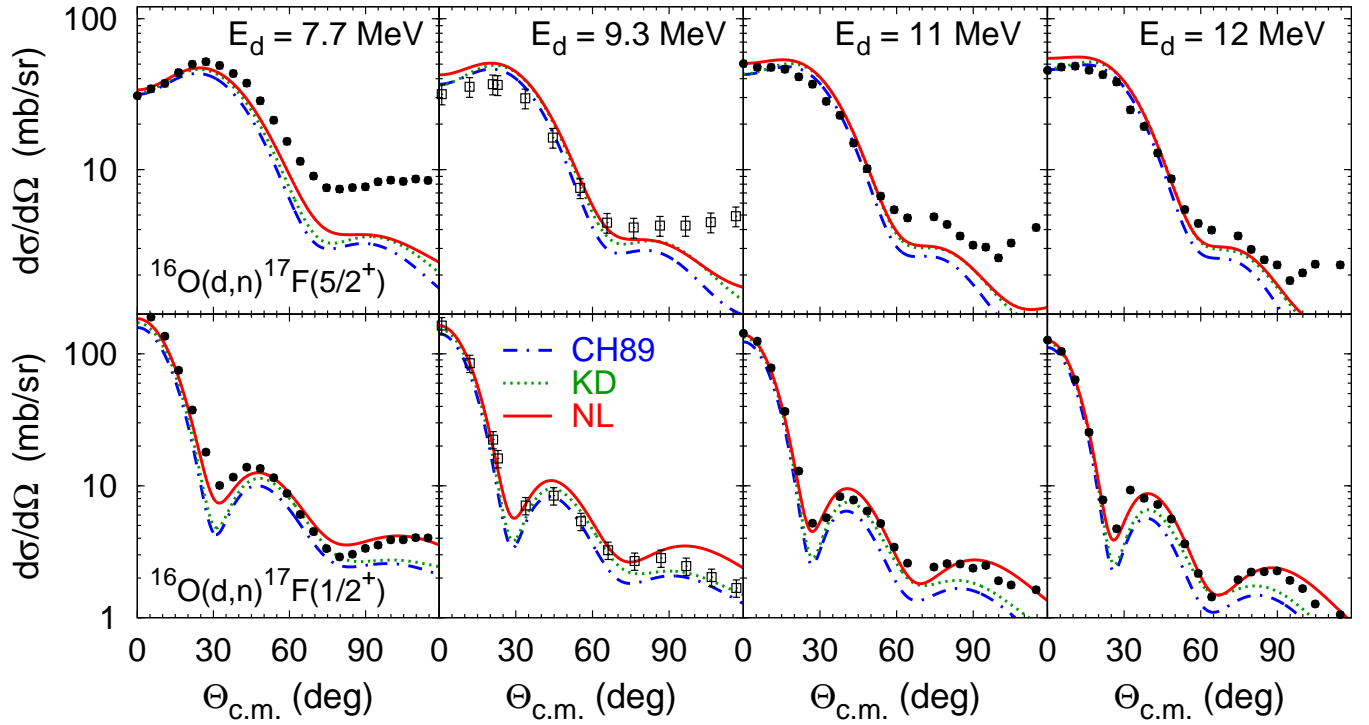


FIG. 5. (Color online) Differential cross section for $^{16}\text{O}(d,n)^{17}\text{F}$ reactions leading to the ^{17}F ground state $5/2^+$ (top) and excited state $1/2^+$ (bottom) at the deuteron energy $E_d = 7.7, 9.3, 11,$ and 12 MeV. Curves are as in Fig. 3, and the experimental data are from Refs. [27] (9.3 MeV) and [28] (other energies).

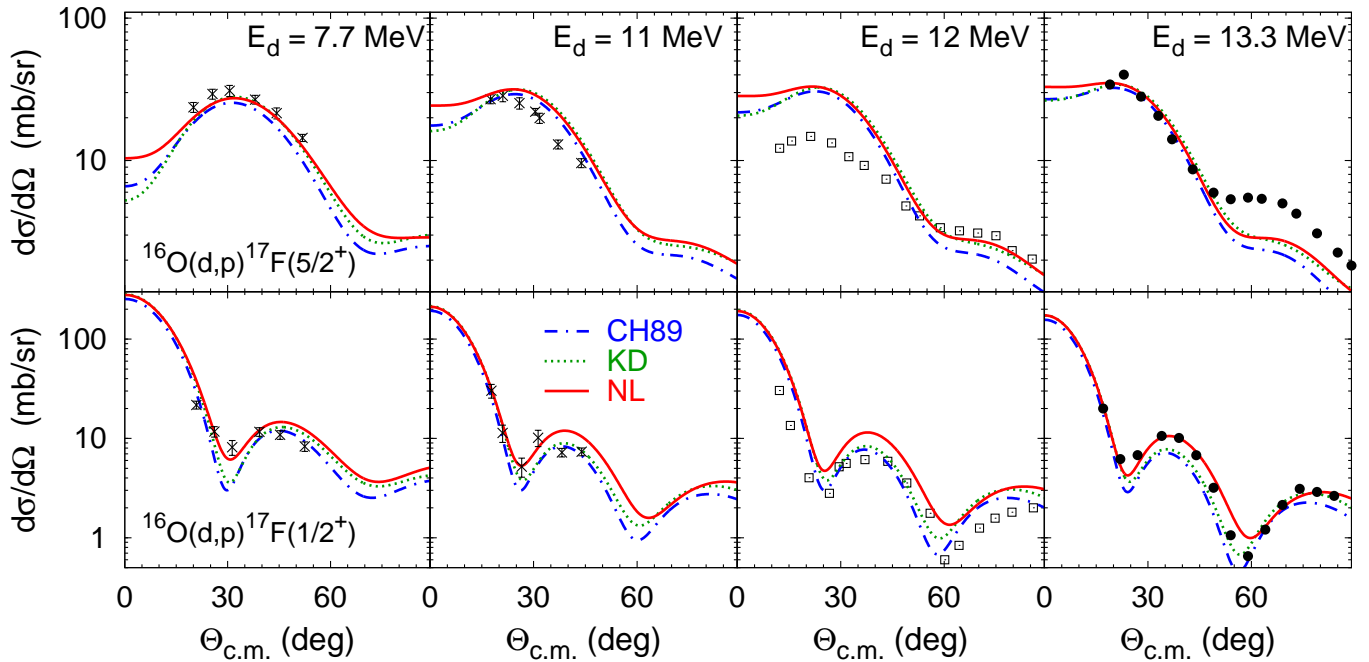


FIG. 6. (Color online) Differential cross section for $^{16}\text{O}(d,p)^{17}\text{O}$ reactions leading to the ^{17}O ground state $5/2^+$ (top) and excited state $1/2^+$ (bottom) at the deuteron energy $E_d = 7.7, 11, 12,$ and 13.3 MeV. Curves are as in Fig. 3, and the experimental data are from Refs. [29] (7.7 and 11 MeV), [30] (12 MeV), and [31] (13.3 MeV).

tunately, the available experimental data for the angular distribution of the cross section, to the best of my knowledge, are limited to low energies $E_d \leq 12$ MeV. The theoretical predictions based on CH89, KD, and NL optical potentials at $E_d = 7.7, 9.3, 11,$ and 12 MeV are presented in Fig. 5 and compared with the experimental data from Refs. [27, 28]. For the transfer to the ^{17}F ground state $5/2^+$ the theoretical results follow the data [28] up to $\Theta_{\text{c.m.}} = 30^\circ$ at $E_d = 7.7$ MeV, up to 60° at $E_d = 11$ MeV, and up to 90° at $E_d = 12$ MeV but underpredict at larger angles. This discrepancy is most sizable at $E_d = 7.7$ MeV, reaching a factor of 2, possibly due to the compound-nucleus reaction mechanism that is expected to become relevant with decreasing energy. The data from Ref. [27] is slightly overestimated at small angles possibly indicating some inconsistency between the two sets [27, 28]. The agreement is better for the transfer to the ^{17}F excited state $1/2^+$. While CH89 and KD results slightly underestimate the data, the nonlocal potential NL reproduces well the experimental data in the whole angular regime up to $\Theta_{\text{c.m.}} = 120^\circ$. This possibly indicates that a simple proton plus core model for the ^{17}F excited state $1/2^+$ is adequate, and supports the conjecture of Ref. [32] on this state being one-proton halo. This is not unexpected given the very weak binding of the $^{17}\text{F}(1/2^+)$ nucleus.

The results for $^{16}\text{O}(d,p)^{17}\text{O}$ reactions at $E_d = 7.7, 11, 12,$ and 13.3 MeV are presented in Fig. 6. The agreement between the theoretical predictions and experimental data [29–31] is almost as good as in the case of Fig. 5, the exception being the $E_d = 12$ MeV data from Ref. [30] whose normalization seems to be inconsistent with the other sets. It is noteworthy that the nonlocal potential NL whose parameters, in contrast to the local potentials CH89 and KD, are independent of the energy, provides a successful description of $^{16}\text{O}(d,p)^{17}\text{O}$ and $^{16}\text{O}(d,n)^{17}\text{F}$ reactions over a broad range of energies (see Ref. [10] for (d,p) reactions at higher energies).

To study the sensitivity of the results to some ambiguities in the chosen Hamiltonian, two additional types of calculations are presented in Fig. 7 for $^{16}\text{O}(d,n)^{17}\text{F}$ reactions at $E_d = 12$ MeV. First, the real binding potential in the nA partial waves with bound states is replaced by the complex NL potential, i.e., the ^{17}O bound states listed in Table I are not supported, and the (d,p) reactions are not taking place. Nevertheless, the results for the (d,n) reactions remain almost unaltered, except at large angles $\Theta_{\text{c.m.}} > 60^\circ$ for the transfer to the ^{17}F excited state $1/2^+$. Second, both nA and pA potentials in the partial waves with bound states are kept real at negative two-body subsystem energies E_α but are taken to be complex NL potentials for $E_\alpha > 0$. Such an abrupt change has been chosen to maximize the possible effect. Although the AGS equations can be solved with such potentials [6], they do not correspond to a definite Hamiltonian, so the conclusions from such calculations have to be taken with care. The effect of the allowed energy-dependence is small for the transfer to the ^{17}F ground state $5/2^+$ up

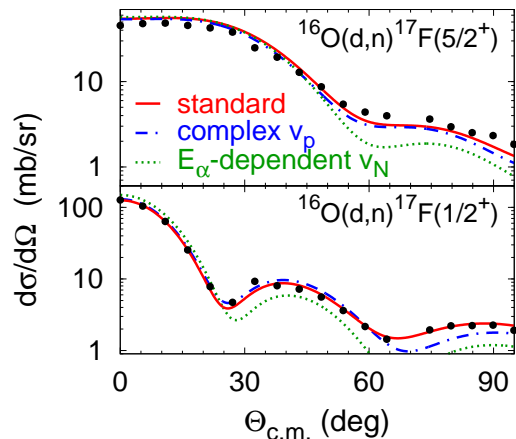


FIG. 7. (Color online) Differential cross section for $^{16}\text{O}(d,n)^{17}\text{F}$ reactions at $E_d = 12$ MeV. Results of standard calculations using the NL potential (solid curves) are compared with the results using the complex nA potential in all partial waves (dashed-dotted curves) and with the results using energy-dependent nA and pA potentials in the partial waves with bound states (dotted curves). The experimental data are from Ref. [28].

to $\Theta_{\text{c.m.}} < 45^\circ$ but is of moderate size for the transfer to the ^{17}F excited state $1/2^+$, even at forward angles. It appears to be correlated with the binding energy. A possible explanation is that the two-body t -matrix pole, located at $E_\alpha = -\epsilon_\alpha$ affects also the $E_\alpha > 0$ region if the binding is weak as in the case of the ^{17}F excited state $1/2^+$. In addition to being non-Hamiltonian, the energy-dependent potential destroys the consistency between the bound state features and threshold behavior that is important in low-energy reactions. The standard calculations of this paper should therefore be considered as more adequate.

IV. SUMMARY

Proton transfer reactions in the deuteron-nucleus collisions were described in a three-body model for the proton + neutron + nuclear core system. The framework of exact integral equations for three-body transition operators as proposed by Alt, Grassberger, and Sandhas was used; they were solved in the momentum-space partial-wave representation. The Coulomb interaction between the proton and the core was included via the screening and renormalization method. The differences relative to the calculation of neutron transfer reactions were pointed out. When the final-state nucleus is weakly bound, e.g., the ^{17}F in the excited state $1/2^+$, the convergence with the screening radius becomes slower for the (d,n) reactions as compared to (d,p) , thereby making the numerical (d,n) calculations more demanding. Nevertheless, well converged results were obtained for the differential cross

section of ${}^7\text{Be}(d, n){}^8\text{B}$, ${}^{12}\text{C}(d, n){}^{13}\text{N}$, and ${}^{16}\text{O}(d, n){}^{17}\text{F}$ reactions.

Realistic CD Bonn potential was used for the interaction between nucleons. In partial waves with the nucleon-core bound states the potential strength was adjusted to reproduce the experimental binding energies while in the other partial waves one of the four optical potentials, i.e., Watson, Chapel Hill 89, Koning-Delaroche, and the nonlocal one by Giannini and Ricco, was used. For the ${}^7\text{Be}(d, n){}^8\text{B}$ reaction the calculations reproduced reasonably the angular shape of the differential cross section data but overpredicted its magnitude, presumably due

to the neglect of the ${}^7\text{Be}$ core excitations. A disagreement with the experimental data in the angular distribution of $d\sigma/d\Omega$ was observed in the ${}^{12}\text{C}(d, n){}^{13}\text{N}$ reaction, similar to earlier findings in the corresponding (d, p) reaction. The description of the ${}^{16}\text{O}(d, n){}^{17}\text{F}$ reactions was quite successful, especially for the transfer to the ${}^{17}\text{F}$ excited state $1/2^+$ using the energy-independent nonlocal optical potential that reasonably reproduced also the ${}^{16}\text{O}(d, p){}^{17}\text{O}$ data over a broader energy range.

This work was supported by the Research Council of Lithuania under contract No. MIP-094/2015.

-
- [1] R. C. Johnson and P. J. R. Soper, Phys. Rev. C **1**, 976 (1970).
- [2] N. Austern, Y. Iseri, M. Kamimura, M. Kawai, G. Rawitscher, and M. Yahiro, Phys. Rep. **154**, 125 (1987).
- [3] L. D. Faddeev, Zh. Eksp. Teor. Fiz. **39**, 1459 (1960) [Sov. Phys. JETP **12**, 1014 (1961)].
- [4] E. O. Alt, P. Grassberger, and W. Sandhas, Nucl. Phys. **B2**, 167 (1967).
- [5] A. Deltuva, A. M. Moro, E. Cravo, F. M. Nunes, and A. C. Fonseca, Phys. Rev. C **76**, 064602 (2007).
- [6] A. Deltuva and A. C. Fonseca, Phys. Rev. C **79**, 014606 (2009).
- [7] J. R. Taylor, Nuovo Cimento B **23**, 313 (1974); M. D. Semon and J. R. Taylor, Nuovo Cimento A **26**, 48 (1975).
- [8] E. O. Alt and W. Sandhas, Phys. Rev. C **21**, 1733 (1980).
- [9] A. Deltuva, A. C. Fonseca, and P. U. Sauer, Phys. Rev. C **71**, 054005 (2005).
- [10] A. Deltuva, Phys. Rev. C **79**, 021602(R) (2009).
- [11] R. Machleidt, Phys. Rev. C **63**, 024001 (2001).
- [12] B. A. Watson, P. P. Singh, and R. E. Segel, Phys. Rev. **182**, 977 (1969).
- [13] R. L. Varner, W. J. Thompson, T. L. McAbee, E. J. Ludwig, and T. B. Clegg, Phys. Rep. **201**, 57 (1991).
- [14] A. J. Koning and J. P. Delaroche, Nucl. Phys. **A713**, 231 (2003).
- [15] M. M. Giannini and G. Ricco, Ann. Phys. (NY) **102**, 458 (1976).
- [16] K. T. Schmitt *et al.*, Phys. Rev. Lett. **108**, 192701 (2012).
- [17] R. C. Johnson and P. J. R. Soper, Nucl. Phys. A **182**, 619 (1972).
- [18] N. K. Timofeyuk and R. C. Johnson, Phys. Rev. C **87**, 064610 (2013).
- [19] W. Liu *et al.*, Phys. Rev. Lett. **77**, 611 (1996).
- [20] J. J. Das *et al.*, Phys. Rev. C **73**, 015808 (2006).
- [21] A. Deltuva, Phys. Rev. C **88**, 011601(R) (2013).
- [22] H. R. Schelin, E. Farrelly Pessoa, W. R. Wylie, E. W. Cybulska, K. Nakayama, L. M. Fagundes, and R. A. Douglas, Nucl. Phys. A **414**, 67 (1984).
- [23] G. S. Mutchler, D. Rendic, D. E. Velkley, W. E. Sweeney Jr., and G. C. Phillips, Nucl. Phys. A **172**, 469 (1971).
- [24] M. A. Kayumov, S. S. Kayumov, S. P. Krekoten, A. M. Mukhamedzhanov, K. D. Razikov, K. Khamidova, and R. Yarmukhamedov, Sov. J. Nucl. Phys. **48**, 403 (1988).
- [25] D. W. Lee, J. Powell, K. Perajarvi, F. Q. Guo, D. M. Moltz, and J. Cerny, J. Phys. G **38**, 075201 (2011).
- [26] J. Lang, J. Liechti, R. Müller, P. A. Schmelzbach, J. Smyrski, M. Godlewski, L. Jarczyk, A. Stralkowski, and H. Witala, Nucl. Phys. A **477**, 77 (1988).
- [27] S. Thornton, Nucl. Phys. A **137**, 531 (1969).
- [28] C. J. Oliver, P. D. Forsyth, J. L. Hutton, G. Kaye, and J. R. Mines, Nucl. Phys. A **127**, 567 (1969).
- [29] I. M. Naqib and L. L. Green, Nucl. Phys. A **112**, 76 (1968).
- [30] J. L. Alty, L. L. Green, R. Huby, G. D. Jones, J. R. Mines, and J. F. Sharpey-Schafer, Nucl. Phys. A **97**, 541 (1967).
- [31] K. W. Corrigan, R. M. Prior, and S. E. Darden, Nucl. Phys. A **188**, 164 (1972).
- [32] R. Lewis and A. C. Hayes, Phys. Rev. C **59**, 1211 (1999).